Co-loading of Levodopa and Curcumin Using Brain-targeted Protocells as a Drug Delivery System for Improving the Efficacy of Parkinson's Disease

wenkai zhou
Chinese Academy of Medical Sciences & Peking Union Medical College Institute of Medicinal Biotechnology https://orcid.org/0000-0002-6589-6384

Chang Liu
Chinese Academy of Medical Sciences & Peking Union Medical College Institute of Medicinal Biotechnology

Feifei Yu
Chinese Academy of Medical Sciences & Peking Union Medical College Institute of Medicinal Biotechnology

Xia Niu
Chinese Academy of Medical Sciences & Peking Union Medical College Institute of Medicinal Biotechnology

Xiaomei Wang
Chinese Academy of Medical Sciences & Peking Union Medical College Institute of Medicinal Biotechnology

Guiling Li (liguiling@imb.pumc.edu.cn)
https://orcid.org/0000-0001-8585-6286

Xinru Li
Peking University School of Pharmaceutical Sciences

Research

Keywords: Parkinson's disease, Levodopa, Curcumin, Brain targeting, Lactoferrin, 58 Mesoporous silica nanoparticle, Protocells

Posted Date: June 29th, 2020

DOI: https://doi.org/10.21203/rs.3.rs-26742/v2

Title page

Co-loading of Levodopa and Curcumin Using Brain-targeted Protocells as a Drug Delivery System for Improving the Efficacy of Parkinson's Disease

Wenkai Zhou[1,2,4], Chang Liu[1,2], Feifei Yu[2], Xia Niu[2], Xiaomei Wang[2], Guiling Li[2]*, Xinru Li[3]*

*Correspondence: liguiling@imb.pumc.edu.cn; ll@bjmu.edu.cn.

[1] Wenkai Zhou, Chang Liu contributed equally to this article.

[2] Institute of Medicinal Biotechnology, Chinese Academy of Medical Science & Peking Union Medical College, Beijing 100050, China.

[3] Department of Pharmaceutics, School of Pharmaceutical Sciences, Peking University, Beijing, China.

[4] Department of Immunology & Centre for Immunotherapy, Institute of Basic Medical Sciences, Peking Union Medical College, Chinese Academy of Medical Sciences, Beijing, China.

Co-loading of Levodopa and Curcumin Using Brain-targeted Protocells as a Drug Delivery System for Improving the Efficacy of Parkinson's Disease

Abstract: Parkinson's disease (PD), one of the most common movement and neurodegenerative disorders, is challenging to treat, partly because the blood-brain barrier blocks passage of most drugs. Levodopa is a common clinical drug for controlling the symptoms of PD, but it only replenishes the missing dopamine, can't protect dopaminergic neurons. While curcumin as a neuroprotective agent has been reported for treatment of PD. Herein, we present a novel organic-inorganic composite nanoparticle with brain targeting (denoted as lf-protocells) for co-delivery of levodopa and curcumin, and demonstrate its attractive use as a biocompatible platform for PD treatment. The nanoparticle system is comprised of a lactoferrin (lf) modified lipid bilayer (LB) containing curcumin as its outer membrane and mesoporous silica nanoparticles (MSNs) containing levodopa as its supporting inner core. Our studies illustrate that the lf-protocells have a size of about 180 nm and spherical morphology, and can be used to co-load levodopa and curcumin efficiently. Further, a cell model and a mouse model induced by rotenone (Rot) and MPTP respectively are used to investigate the effects of binary-drug loaded lf-protocells on PD. Our results demonstrate that the combination of curcumin and levodopa alleviate the apoptosis of PD cells, enhance the cell viability as compared to levodopa used alone; levodopa together with curcumin also efficiently decrease the expression of a-synuclein,

increase the expression of tyrosine hydroxylase in SH-SY5Y cells, and transform more levodopa into dopamine for supplement the loss of the brain. Moreover, the resulting binary-drug loaded lf-protocells ameliorate oxidative stress and mitochondrial dysfunction as compared to combination of free drugs. In addition, testing in a mouse model indicate that lf-protocells can improve significantly the motor function and distribution in brain compared with unmodified protocells. In conclusion, binary-drug loaded lf-protocells show much better therapeutic efficacy in both the cell model and the mouse model of PD and lower toxicity than bare MSNs. These results suggest that lf-protocells can be used as a promising drug delivery platform for targeted therapy against PD and other diseases of the central nervous system.

Keywords: Parkinson's disease, Levodopa, Curcumin, Brain targeting, Lactoferrin, Mesoporous silica nanoparticle, Protocells

1. Background

Parkinson's disease (PD) is the second most common chronic progressive neurodegenerative disorder after Alzheimer's disease (AD) as it affects almost 1-2% of population aged over 65 in the world [1]. The typical pathological hallmarks of PD include the loss of dopaminergic neurons in the substantia nigra pars compacta (SNc) and the appearance of Lewy bodies formed by the accumulation of misfolded α-synuclein (α-syn) protein. Although the pathogenesis of PD is still unknown [2],

most reports show that it is associated with oxidative stress, neuro inflammatory reaction, mitochondrial dysfunction, cell apoptosis and so on [3-9].

So far, levodopa is considered the most effective medication for the symptomatic treatment of PD [10]. It works by being converted into dopamine and compensating for the dopamine deficiency in the brain. However, the efficacy of levodopa in the late stage of PD is significantly reduced due to its metabolism, subsequent low bioavailability and irregular fluctuations of its blood concentration [11]. Furthermore, levodopa, only as a neurotransmitter supplement, cannot effectively prevent or delay the deterioration of PD. It is noted that several drug candidates such as EPI-743, Baicalein and NTCELL currently used in clinical trials exert their therapeutic effects on PD by antioxidation, protecting mitochondria or acting on glial cells. It suggests that intervention of oxidative stress, improvement of mitochondrial dysfunction, resistance to neuroinflammation, protection of dopamine and other nerve cells are potential therapeutic strategies for PD [12].

As a natural polyphenol extracted from the dry rhizome of zingiberaceae plants [13], curcumin has numerous pharmacological properties such as anti-inflammation, antioxidation, anti-tumor and anti-nerve degeneration [14, 15]. It reduces the high level of oxidative stress and neurotoxicity mainly through antioxidant effect and chelating metal ions, and thus achieves the protection of dopaminergic neurons and improves the level of dopamine [16-19]. Previous studies suggested that curcumin could be applied in the treatment of neurodegenerative diseases such as PD and AD [20, 21]. Hence, if combined with levodopa, curcumin may lead to enhanced

therapeutic effects of PD on the basis of levodopa supplementing neurotransmitters, since it works through antioxidation and repairing injured neurons. In other words, the combination of these two different durgs is expected to enhance the therapeutic effect of PD. So far, no relevant pharmacological study has been reported.

However, the physicochemical properties of hydrophilic levodopa and hydrophobic curcumin are quite different, which make their co-delivery confront with great challenges. It is necessary to construct an eligible drug delivery system that efficiently co-load these two drugs. Protocells, consisting of a mesoporous silica nanoparticles (MSNs) core coated by a layer of lipid bilayer (LB), are a class of highly scalable nanocarriers that have caused great concern in drug delivery applications [22, 23]. Inner sponge-like inorganic MSNs with favorable surface area, high porosity and adsorption performance, extraordinary drug loading capacity, are excellent carriers of hydrophilic drugs such as levodopa. The outer membrane LB can not only contain hydrophobic drugs like curcumin but also effectively seal the surface pores of the inner MSNs to prevent drug leakage, thus achieving the co-delivery of the different drugs [23-27]. In addition, these drugs can be delivered simultaneously without affecting each other.

In our study, protocells delivery system co-loaded with levodopa and curcumin were constructed. In addition, brain targeting ligand-lactoferrin (Lf) was modified on the LB surface to enhance cellular uptake and brain targeting [28]. The blood–brain barrier (BBB), formed by brain vessel endothelial cells linked together with tight junctions. This cellular interface helps to maintain a steady, optimal environment for

neuronal function, and selective transport systems regulate the transport of wanted molecules. But on the other hand, it presents a major obstacle to the delivery of drugs passing from the bloodstream to the central nervous system (CNS) [29]. Lf receptor existing on the BBB mediated endocytosis is among the most efficient cellular uptake pathway. The delivery system with Lf attachment may be more efficient under certain pathological conditions of the high expression of Lf receptor, such as PD [30] and AD [31].

The physicochemical properties, efficacy *in vitro*, mechanism of action and preliminary pharmacodynamics *in vivo* of the drug delivery system named as binary-drug loaded lf-protocells (L/C-Lf-Pro) were investigated. These results are expected to offer a beneficial strategy in mitigating the adverse reaction of levodopa and improving the therapeutic effect, and have the potential to provide a new approach for the development of drug delivery system with high-efficiency and important application prospect for curing PD.

2. Materials and methods

2.1 Materials

Tetraethyl orthosilicate (TEOS, 98%), cetyltrimethylammonium bromide (CTAB, > 99%), Brij-58, 5,5'-dithiobis-2-nitrobenzoic acid (DTNB) and 2-iminothiolane hydrochloride (Traut's reagent) were purchased from Aladdin-chemistry (Shanghai, China). Lactoferrin was obtained from China Peptides Co. (Shanghai, China). 1,3,5-trimethylbenzene (TMB) and curcumin were purchased

from Alfa Aesar (Shanghai, China). 3-(4,5-Dimethylthiazol-2-yl)-2,5-diphenyltetrazolium bromide (MTT) and rhodamine 123 (Rh123) were purchased from Sigma Aldrich (USA). Cy5-SE was from MedChemExpress (USA). Triton X-100 was from Beijing Innochem Science & Technology Co., Ltd (Beijing, China). Total Superoxide Dismutase Assay Kit with WST-8, GSH and GSSG Assay Kit, primary antibody dilution buffer, transfer buffer and BeyoECL Moon were purchased from Beyotime Institute of Biotechnology (Shanghai, China). DMEM/F-12 medium, fetal bovine serum (FBS), penicillin-streptomycin and phosphate buffer saline (PBS) were purchased from Corning (USA). 1,2-distearoyl-*sn*-glycero-3-phosphoethanolamine-N-[methoxy(polyethyleneglycol)-2000] (DSPE-PEG_{2000}), 1,2-distearoyl-*sn*-glycero-3-phosphoethanolamine-N-[maleimide(polyethylene glycol)-2000] (DSPE-PEG_{2000}-MAL), dipalmitoyl phosphatidylcholine (DPPC) and cholesterol (Chol) were purchased from A.V.T. Pharmaceutical Co., Ltd (Shanghai, China). Rotenone (Rot), 1-methyl-4-phenyl-1,2,3,6-tetrahydropyridine (MPTP), borate-EDTA buffer, Rhodamine B isothiocyanate (RBITC), (3-Aminopropyl) triethoxysilane (APTES) and SDS-PAGE running buffer were purchased from Dalian Meilun Biotechnology Co., Ltd (Dalian, China). Levodopa (>98%) was purchased from Beijing Innochem Science & Technology Co., Ltd (Beijing, China). DAPI, Reactive Oxygen Species Assay Kit, BCA Protein Assay Kit, RIPA buffer, SDS-PAGE Gel Kit, loading buffer (with DTT, 4X) and Color Mixed Protein Marker

were obtained from Beijing Solarbio Science & Technology Co., Ltd (Beijing, China). Anti-β-actin, anti-GAPDH, anti-α-synuclein and anti-tyrosine hydroxylase (TH) antibodies were obtained from Proteintech, USA. Anti-Bcl-2, anti-Bax, anti-Caspase-3 and anti-PARP antibodies were received from Cell Signaling Technology, USA. Secondary antibodies HRP-conjugated Affinipure Goat Anti-Mouse IgG(H+L) and Anti-Rabbit IgG(H+L) were obtained from Proteintech, USA. Deionized water was used in all experiments and analyses. All other chemicals were reagent grade and used directly without further purification or modification.

2.2 Cell culture and treatments

SH-SY5Y cells (purchased from the Ke Lei Biological Technology Co., Ltd.) were maintained in DMEM/F-12 medium containing 10% fetal bovine serum (FBS), 1% antibiotic cocktail of penicillin-streptomycin at 37 ℃ under an atmosphere of 5 % CO_2 and 90 % relative humidity.

The SH-SY5Y cells were subsequently divided into 8 experimental groups: (1) the control group: DMEM/F-12 medium alone, (2) the rotenone group: rotenone solution alone (Rot), (3) the curcumin group: 2 μM curcumin (C) + Rot, (4) the levodopa group: 40 μM levodopa (L) + Rot, (5) the levodopa and curcumin group: (40 μM levodopa + 2 μM curcumin) (free L/C) + Rot, (6) the curcumin-loaded lf-protocells group: 2 μM curcumin-loaded lf-protocells (C-Lf-Pro) + Rot, (7) the levodopa-loaded lf-protocells group: 40 μM levodopa-loaded lf-protocells (L-Lf-Pro) + Rot, and (8) the levodopa/curcumin co-loaded lf-protocells group: (40 μM levodopa

+ 2 μM curcumin)-loaded lf-protocells (L/C-Lf-Pro) + Rot. The molar concentration of levodopa and curcumin loaded in C-Lf-Pro, L-Lf-Pro or L/C-Lf-Pro group were equivalent to corresponding free drug group.

2.3 Animals

The male C57BL/6 mice (10 weeks old) and male BALB/c nude mice (initial weight of 18–20 g) provided by SPF (Beijing) Biotechnology Co., Ltd were kept under specific-pathogen-free condition. All animal experimental procedures were performed in accordance with guidelines approved by the ethics committee of Chinese Academy of Medical Science & Peking Union Medical College. Mice had free access to standard chow diet and water and were maintained in plastic cages filled with hardwood chips in a temperature-controlled room (24 ℃) on a 12:12 h light/dark cycle for 7 days prior to the experiments.

2.4 Synthesis of MSNs

Various mesoporous silica nanoparticles were prepared according to the literature with little modification [32]. In brief, 0.437 g of CTAB and 0.472 g of Brij58 were dissolved in 100 mL of 0.1 M phosphate buffer solution (pH=7.4). With vigorous stirring for 20 min at 60 ℃, 2.14 ml of TEOS was added to the solution at a rate of approximately 30 drops per minute, and the stirring process at 60 ℃ was continued for another 8 h. In order to enlarge the pore size to increase adsorption, 2 ml of TMB was added after the addition of TEOS for 40 min. Then, the stirring process at 60 ℃

was continued for another 8 h. To distinguish, we called the product synthesized without adding TMB as small pore MSNs (sp-MSNs), while synthesized with adding TMB as MSNs. The resulting white precipitate of sp-MSNs or MSNs was purified to remove remaining surfactant by centrifugation and washed with ethanol and water three times each. To remove the organic template, the sediment was refluxed for 24 h at 78 ℃ in acidic ethanolic solution (ethanol: hydrochloric acid (HCl) = 60:1, v/v). And the resulting white precipitate was purified by centrifugation and washed with ethanol for three times.

2.5 Characterization of sp-MSNs and MSNs

For measuring particle size distribution such as mean particle size as well as PDI, sp-MSNs and MSNs were diluted to an appropriate volume with distilled water and measured by the dynamic light scattering (DLS) method (Malvern Instruments, UK) at room temperature. The nitrogen adsorption/desorption analysis was performed using an adsorption analyzer (ASAP 2460, Micromeritics, USA). According to the adsorption data, the Brunauer-Emmett-Teller (BET) and Barrett-Joyner-Halenda (BJH) models were used to calculate the specific surface areas and the pore size of sp-MSNs and MSNs. Morphology of sp-MSNs and MSNs were observed via transmission electron microscopy (TEM, JEM-100CX II, JEOL, Japan).

2.6 Preparation of lf-protocells and drug loading

Refer to Huan Meng's synthetic method of protocells, the lipid bilayer (LB)

coating with MSNs were achieved as follow [33]. The coating lipid bilayer consisted of a DPPC/Chol/DSPE-PEG_{2000} mixture, the molar ratio of which was 75:20:5. These three excipients were dissolved in chloroform and placed into a round-bottom flask, the resulting lipid solution was dried to a film by a rotary vacuum evaporator (RV10 digital, IKA, Germany) for 15 min at room temperature. Following the addition of 2 mL MSNs suspension to the as-prepared coating lipid film at a ratio of 1:1 (w/w dry weight), probe sonication was used for 15 min with 15/15 s on/off working cycle at a power output of 50 W. Since the resulting suspension contained protocells, liposomes and others, the protocells were separated by centrifugation at 12000 rpm for 10 min, followed by washing three times in saline.

Lactoferrin modified protocells (denoted as lf-protocells) were prepared according to a previously described method with slight modifications [28]. Lactoferrin (Lf) was dissolved in borate-EDTA buffer (pH 8.0) containing Traut's reagent for 2 h at 4℃. The obtained Lf-SH was mixed with DSPE-PEG_{2000}-MAL in PBS (pH 7.0) for 24 h under constant shaking in the dark at 4℃. Thereafter, the product was dialyzed and freeze-dried to acquire the conjugate DSPE-PEG_{2000}-Lf in powder form. The coating lipid bilayer consisted of a DPPC/Chol/DSPE-PEG_{2000}/DSPE-PEG_{2000}-Lf mixture, the molar ratio of which was 75:20:4:1. Finally, lf-protocells were obtained according to the above preparation method of protocells.

To obtain levodopa-soaked MSNs, levodopa was dissolved in HCl (pH 1.0) with a concentration of 10 mg/mL, then 10 mg of MSNs were soaked in 2 mL of levodopa

243 solution for 48 h under light-sealed condition at room temperature.

244 To obtain curcumin loaded lipid film, 200 μg curcumin was added to the mixed
245 lipid solution followed by rotary evaporation drying to form the lipid film containing
246 curcumin.

247 To achieve co-loading of levodopa/curcumin, the levodopa-soaked MSNs
248 suspension was added to the lipid film containing curcumin, followed by rehydration,
249 sonication, centrifugation, and washing, similar to preparation method of protocells
250 described above. The Fig. 1A depicted the preparation procedure for lf-protocells as a
251 carrier for delivery of a combination of levodopa and curcumin.

252

253 2.7 Characterization of lf-protocells

254 The conjugate DSPE-PEG_{2000}-Lf was identified by ^{1}H-NMR spectroscopy.
255 DSPE-PEG_{2000}-MAL and DSPE-PEG_{2000}-Lf were dissolved in D_2O and analyzed in a
256 ^{1}H-NMR spectrometer (Bruker, Switzerland).

257 For measuring particle size distribution such as mean particle size and PDI of
258 various lf-protocells (unloaded and drugs-loaded), nanoparticles were diluted to an
259 appropriate volume with distilled water and measured by the DLS method (Malvern
260 Instruments, UK) at room temperature. Unloaded and drugs-loaded lf-protocells were
261 characterized for morphology using a TEM (JEM-100CX II, JEOL, Japan). A
262 minimum of three images for each sample was captured.

263

264 2.8 Encapsulation efficiency and drug loading content of lf-protocells

The encapsulation efficiency (EE) and drug loading content (DLC) of drug-loaded lf-protocells were determined by a subtraction method as the following equations:

$$EE(\%)=\frac{(\text{total mass of drug in loading})-(\text{the mass of non-encapsulated drug})}{\text{total mass of drug in loading}}\times 100$$

$$DLC(\%)=\frac{(\text{total mass of drug in loading})-(\text{the mass of non-encapsulated drug})}{\text{total mass of MSNs}}\times 100$$

The concentration of levodopa was determined by high-performance liquid chromatography (HPLC) with the mobile phase composed of tetrahydrofuran and 0.1 % TFA (3:97, v/v), and UV detection operated at 280 nm; while the concentration of curcumin was determined by HPLC with the mobile phase composed of methanol and 4 % acetic acid (75:25, v/v), and UV detection operated at 430 nm.

2.9 Hemolysis assay of MSNs and lf-protocells

Hemolysis assays were used to assess the safety of MSNs and lf-protocells for *in vivo* applications. After collection of beagle dog blood samples, red blood cells (RBCs) were collected by centrifugation at 1000 rpm for 10 min. After discarding the supernatant and washing three times with sterile isotonic saline, the RBCs suspension was diluted to a concentration of 2 % (v:v). Subsequently, 0.4 mL of 2 % RBCs suspensions were mixed with 0.8 mL of MSNs (or lf-protocells) suspensions in saline at 50, 100, 200, 400, 600, 800, and 1000 μg/mL concentration. The hemolysis of RBCs in saline and 5 % Triton X-100 served as negative and positive control, respectively. The mixtures were incubated at 37 ℃ for 1 h and then centrifuged at 1000 rpm for 3 min. The supernatants were measured at 540 nm using a microplate

285 reader (BioTek Synergy H1, USA). The following formula was used to calculate the
286 hemolysis percentage:

287 $$\text{Hemolysis percentage (\%)} = \frac{(\text{absorbance of the sample - absorbance of the negative control})}{(\text{absorbance of the positive control - absorbance of the negative control})} \times 100$$

288

289 2.10 *In Vitro* cell proliferation and viability by MTT assay

290 Cellular toxicity of nanoparticles was determined using a colorimetric assay with
291 MTT. SH-SY5Y cells were seeded in 96-well plates (1×10^4 per well) and incubated
292 for 24 h. Subsequently, cells were exposed to various concentrations of MSNs or
293 lf-protocells for an additional period of 24 h. Cell viability assays were then
294 determined by MTT.

295 Protection effects of free drug and drug-loaded lf-protocells against
296 rotenone-induced cytotoxicity were also determined using a colorimetric assay with
297 MTT. SH-SY5Y cells were cultured in 96-well plates (1×10^4 per well) for 24 h.

298 To determine the toxicity of rotenone, SH-SY5Y cells were incubated with
299 different concentrations of rotenone (0.5, 1, 2, 4, 10 and 20 μM) for 24 h. After
300 co-incubated for 24 h, cell viability assays were then determined by MTT.

301 To determine the neuroprotective effects of free drugs (levodopa and curcumin),
302 SH-SY5Y cells were pretreated with free drug. A series of concentrations of curcumin
303 were 1, 2, 4 μM and the concentrations of levodopa were 20, 40 μM. Then these cells
304 were treated with 4 μM rotenone. After co-incubated for 24 h, cell viability assays
305 were then determined by MTT.

306 To determine the neuroprotective effects of drug-loaded and unloaded

lf-protocells, SH-SY5Y cells were pretreated with these lf-protocells. Then the cells were treated with 4 μM rotenone. After co-incubated for 24 h, cell viability assays were then determined by MTT.

For the MTT assay, each well was treated with 100 μl of MTT-labeling reagent (0.5 mg/ml), and the plate was incubated for an additional 3 h. The resulting formazan crystals were dissolved with 150 μl of dimethyl sulfoxide, and MTT reductions were detected at 595 nm by the microplate reader (BioTek Synergy H1, USA).

2.11 Oxidative stress detection

2.11.1 Measurement of intracellular reactive oxygen species (ROS)

In order to determine the cellular ROS level, Reactive Oxygen Species Assay Kit was used. Intracellular ROS level was measured by 2', 7'-dichlorofluorescein diacetate (DCFH), which can be oxidized into fluorescent DCF. SH-SY5Y cells (about 1×10^5 cells/well in 6-well plates) were cultured for 24 h. After treatment as described in part 2.2 above for 24h, cells were washed twice with PBS and then incubated with 4 μM DCFH-DA in the dark for 20 min. Cells were washed twice with PBS and harvested in trypsinization. All samples were measured via FACS calibur flow cytometer (BD, USA). Fluorescent measurements were done with excitation and emission wavelengths set at 488 nm and 525 nm, respectively. The experiment was repeated in triplicate.

2.11.2 Measurement of intracellular superoxide dismutase (SOD) activity

The SOD activity was quantified by Total Superoxide Dismutase Assay Kit with WST-8. SH-SY5Y cells were seeded in a 6-well plate at 1×10^5 cells/well and treated for 24h as described in part 2.2 above. Cells were harvested and washed twice with PBS. Then, the SOD activity of the sample was determined according to the manufacturer's instructions, and the absorbance value was read at 450 nm by the microplate reader (BioTek Synergy H1, USA). The protein content was determined using the BCA protein assay. Each experiment was performed in triplicate.

2.11.3 Determination of cellular total glutathione (GSH) level

The total GSH level was quantified by GSH and GSSG Assay Kit. SH-SY5Y cells were seeded in a 6-well plate at 1×10^5 cells/well and treated as described in part 2.2 above. After 24 h incubation, cells were collected and washed twice with PBS. Then each sample was mensurated according to the manufacturer’s instructions. Then, the absorbance value was measured at 412 nm by the microplate reader (BioTek Synergy H1, USA). Each experiment was performed in triplicate.

2.12 Measurement of mitochondrial membrane potential (MMP)

To monitor the MMP changes of cultured cells, the mitochondrial specific fluorescent dye Rh123 was used. SH-SY5Y cells were plated in 6-well plates for the treatment listed in part 2.2 above. After 24 h incubation, the medium of each sample was removed, then 1 mL FBS-free medium with 1 μM Rh123 was added in, the incubation was continued for 30 min in the dark at 37 °C. Data were analyzed using a

flow cytometer (BD Biosciences, USA).

To visualize the mitochondrial function of cultured cells, the medium was removed after 24 h incubation. Each sample was incubated with 1 μM Rh123 for 30 min in the dark at 37 °C. Then cells were washed twice with PBS and photographed immediately using an Ultra High Resolution Microscope (TCS SP8 STED, Leica, Germany). The results were expressed as mean Rh123 fluorescence intensity. The experiment was repeated in triplicate.

2.13 Western blot

SH-SY5Y cells were lysed in RIPA lysis buffer supplemented with protease inhibitors. After quantified by BCA protein assay, samples were mixed with loading buffer (containing DTT) at a ratio of 4:1, and then boiled for 10 min. The resulting proteins were separated with SDS-PAGE and transferred onto a PVDF membrane. Then the membrane was sealed up in TBST with 5 % skim milk at room temperate for 2 h, and subsequently cultured with primary antibodies including anti-TH, anti-α-synuclein, anti-Bcl-2, anti-Bax, anti-Caspase-3, anti-PARP, anti-β-actin and anti-GAPDH at 4 °C overnight. After TBST-washing in triplicate, the membrane was incubated with secondary antibody HRP-conjugated Affinipure Goat Anti-Mouse IgG(H+L) and Anti-Rabbit IgG(H+L) for 1 h at room temperature. Protein bands were visualized using enhanced chemiluminescence. The results were analyzed by Image J. GAPDH and β-actin were included as internal controls. The experiment was repeated in triplicate.

2.14 Cellular uptake

To investigate the uptake behavior of protocells (unmodified with Lf) and lf-protocells, fluorescence-labeled protocells and lf-protocells (denoted as RBITC/Calcein-protocells and RBITC/Calcein-lf-protocells, respectively) with RBITC-conjugated and Calcein-soaked MSNs as the inner cores were prepared.

For RBITC-conjugation, 8.6 mg RBITC and 200 μL APTES were dissolved in 2mL absolute ethanol. The solution reacted for 24h in the dark under stirring. RBITC-conjugated MSNs were prepared as follow: CTAB, Brij58 and TEOS were added as described above. After that, 200 μL of the reacted solution was added. The following procedures were the same as the synthetic method of MSNs. For Calcein-soak, Calcein was soaked following a similar approach of levodopa-soaked MSNs, as described above. RBITC/Calcein-protocells and RBITC/Calcein-lf-protocells were prepared refer to synthetic method of protocells as described above.

For cellular uptake assay, bEnd.3 cells were seeded on glass bottom dishes at a density of 5×10^4 cells/mL per chamber and incubated for 24 h under an atmosphere of 5 % CO_2 at 37 ℃. The cells were then treated with 200 μg/mL RBITC/Calcein-protocells or RBITC/Calcein-lf-protocells for 4 h. After washing three times with PBS, the cells were treated with 4 % paraformaldehyde for 30 min at 4 ℃ and the nucleus were subsequently labeled with DAPI. After that, the dishes were visualized under Ultra High Resolution Microscope (TCS SP8 STED, Leica,

Germany). The fluorescence intensity of RBITC was determined with an excitation wavelength of 540 nm and an emission wavelength of 625 nm. The fluorescence intensity of Calcein was determined with an excitation wavelength of 496 nm and an emission wavelength of 515 nm.

2.15 *In Vivo* Study

2.15.1 Biodistribution

To investigate the biodistribution behavior of lf-protocells in mouse, fluorescence -labeled lf-protocells denoted as Cy5-lf-protocells were prepared using Cy5-conjugated MSNs as the inner core. For synthesis of Cy5-conjugated MSNs, 2.5 mg Cy5-SE and 200 μL APTES were dissolved in 2mL DMSO. The solution reacted for 24h in the dark under stirring. Cy5-conjugated MSNs were prepared as follow: CTAB, Brij58 and TEOS were added as described above. After that, 200 μL of the reacted solution was added. The following procedures were the same as the synthetic method of MSNs.

The male BALB/c nude mice (n=3) were given 200 μL of 5mg/ml Cy5-labeled lf-protocells via intraperitoneal injection. Then, the mice were anesthetized by isoflurane inhalation and scanned in an IVIS Spectrum CT system (Maestro2, CRI, USA) at various time points. The images of the mice were collected at an excitation wavelength of 649 nm and an emission wavelength of 670 nm.

2.15.2 Open-Field Test

Male C57BL/6 mice were randomly assigned to six groups (n = 8/group):

One group were treated with saline only (Control). PD model mice were induced by MPTP, received intraperitoneal (i.p.) injections of MPTP (20 mg/kg/day) for 5 days (MPTP). Various therapeutic groups were treated with 20 mg/kg free levodopa (L), 20 mg/kg free levodopa + 2 mg/kg free curcumin (free L/C), levodopa/curcumin co-loaded protocells (L/C-Pro, encapsulated with 20 mg levodopa and 2 mg curcumin), and levodopa/curcumin co-loaded lf-protocells (L/C-Lf-Pro, encapsulated with 20 mg levodopa and 2 mg curcumin) respectively using i.p. injections at 1 h before MPTP treatment for 5 days [34].

To evaluate the exploratory and locomotor activities by Open-Field Test, each mouse was placed into the center of a square open-field box (24 cm * 24 cm * 10 cm, divided into sixteen squares with grids, made of transparent PVC) and acclimated for 10 min. The motor function of each mouse was evaluated by counting the number of line crossings during 5 min in the square open-field box, persist for five days [34].

2.16 Data processing

All data were presented as mean ± SEM (standard error of mean) of triplicates measurement. All statistical analysis was done in Graph Pad Prism software. Statistical differences between groups were evaluated using a two-tailed Student's t test and differences with a $P < 0.05$ were considered significant.

3. Results and discussion

3.1 Characterization of sp-MSNs and MSNs

MSNs nanoparticles were synthesized by the sol-gel phase transition method, in which TEOS was used as a silica source, CTAB and Brij-58 as the structure-directing agents [32]. With a slight modification, TMB was used for enlarging pores to provide a higher loading capacity [35].

The DLS test indicated that the prepared MSNs had outer diameter about 90 nm, similar like the sp-MSNs without TMB modification (Tab S1). TEM images showed that, the prepared MSNs retained the high monodispersity and spherical morphology, and meanwhile possessed larger porosity compared with the sp-MSNs without TMB modification (Fig. S1). According to nitrogen adsorption data, with the enlarging pores modification, the BET surface area, pore volume, and pore size were changed from 743.78 m^2/g, 1.01 cm^3/g, and 5.44 nm to 572.99 m^2/g, 1.15 cm^3/g, and 8.00 nm respectively (Fig. S2, Tab. S2).

3.2 Characterization of lf-protocells and drug loading

As for ^{1}H-NMR spectra analysis, the solvent peak of D_2O at δ 4.71 ppm was used as the reference (Fig. 1B). The ^{1}H-NMR spectrum of DSPE-PEG_{2000}-MAL clearly showed characteristic peak of MAL group at δ 6.84 ppm (Fig. 1B), while the disappearance of MAL peak in the ^{1}H-NMR spectrum of DSPE-PEG_{2000}-Lf (Fig. 1B) matched well with the fact that the MAL group had been reacted with the thiol group of Lf-SH. The ^{1}H-NMR spectrum demonstrated the formation of DSPE-PEG_{2000}-Lf.

The DLS test indicated that lf-protocells were larger than MSNs, up to 177 nm in

diameter. The presence of the coating lipid bilayer was confirmed by TEM. As can be seen, the lf-protocells appeared to be surrounded by a ring, and the appearances of the pores were relatively vague compared with TEM image of MSNs shown in Fig. S1. The co-loading of levodopa and curcumin had little influence on the morphology of lf-protocells (Fig. 1C).

And the results of DLC and EE of various lf-protocells were shown in Tab. 1. L-Lf-Pro yielded a levodopa DLC of 21.59 wt % (drug: MSNs) and a levodopa EE of 10.80 wt %, which were quite similar to that of binary-drug loaded lf-protocells (DLC of 20.28 wt % and EE of 10.14 wt % for levodopa).

As previously mentioned, hydrophobic drug, such as curcumin, could be loaded in the outer membrane LB and have a synergistic effect with levodopa to treat Parkinson's disease in theory.

HPLC analysis indicated that the C-Lf-Pro yielded a curcumin DLC of 1.93 wt % (drug: MSNs) and a curcumin EE of 96.57 wt %, which were also quite similar to that of binary-drug loaded lf-protocells (DLC of 1.97 wt % and EE of 98.32 wt % for curcumin).

The co-loading of levodopa and curcumin showed a similar DLC and EE value to that of single-drug loaded lf-protocells, which was attributable to the possible deep immersion of levodopa in the MSNs core and the immersion of curcumin in the lipid bilayer.

In addition, the in vitro release profiles of levodopa and curcumin from binary-drug loaded lf-protocells in neutral or acidic medium were measured using

HPLC (Fig. S3). Neutral medium of pH 7.4 simulated body fluid, and acidic medium of pH 5.0 simulated endosomal/lysosomal environment. The results suggested that no levodopa and only 59.2% curcumin was released from lf-protocells for 48 h in pH 7.4 solution at 37 °C. When the pH is decreased to acidic condition (pH 5.0), lf-protocells released 100.4% of their curcumin and 72.6% of their levodopa within 48 hours. Therefore, we speculated that the release of levodopa was hindered by the inclusion of lipid bilayer outside the inner core, which would greatly reduce its leakage in the circulatory system. However, the drug release from lf-protocells in acidic conditions is initiated by LB destabilization.

Fig. 1 Preparation and characterization of lf-protocells of lf-protocells.

(**A**) Scheme of the preparation of lf-protocells as a carrier for co-delivery of levodopa and curcumin. (**B**) ^{1}H-NMR spectra of DSPE-PEG$_{2000}$-MAL (top) and DSPE-PEG$_{2000}$-Lf (bottom) (D_2O as the solvent). (**C**) TEM images of various lf-protocells. (1) unloaded lf-protocells; (2) levodopa loaded lf-protocells; (3) curcumin loaded lf-protocells; (4) binary-drug loaded lf-protocells.

Tab 1. Physicochemical characteristics of various Lf-Protocells (mean ± SD; n=3).

	unloaded Lf-Protocells	levodopa loaded Lf-Protocells	curcumin loaded Lf-Protocells	binary-drug loaded Lf-Protocells	
				levodopa	curcumin
Particle size	176.2 ± 1.4	226.8 ± 5.4	207.6 ± 0.8	219.3 ± 7.2	

(nm)					
PDI	0.176 ± 0.002	0.154 ± 0.005	0.205 ± 0.007	0.149 ± 0.005	
EE (%)	—	9.87 ± 0.38	86.67 ± 0.12	10.72 ± 0.04	88.31 ± 0.02
DLC (%)	—	20.89 ± 0.34	1.73 ± 0.02	21.44 ± 0.09	1.89± 0.01

3.3 Biocompatibility and cytotoxicity of MSNs and lf-protocells

Hemolysis and cell viability assays were performed to investigate biocompatibility and cytotoxicity of MSNs (as the inner core of lf-protocells) and lf-protocells.

The hemocompatibility of MSNs, protocells and lf-protocells was evaluated by hemolysis assay at the concentrations ranging from 50 to 1000 μg/mL. The hemolytic activity of MSNs, protocells and lf-protocell on RBCs was observed using digital photography and calculated by the formula of hemolysis percentage as described above (Fig. S4). Visual inspection of the hemolysis experiments showed a clear color differential between samples with varying degrees of hemolysis. Uncoated MSNs showed high hemolytic activity, roughly 40 % of the positive hemolysis control of RBCs when the concentration exceeded 400 μg/mL. In contrast, with the lipid bilayer (LB) coating, protocells showed the hemolytic activity below 5 % of the positive hemolysis control of RBCs, even at concentrations greater than 800 μg/mL. In addition, the hemolysis ratio of lf-protocells with a concentration of 1000 μg/mL was still less than 5 % compared with the positive control group. Studies on other particle systems have determined that increasing the positive charge density of the particle

519 leads to a decrease in hemolysis. When acidic silanols on MSNs have been masked by
520 the lipid bilayer, no hemolysis is observed [36]. This result demonstrated that the LB
521 coating on the surface of MSNs could improve markedly the biocompatibility of silica,
522 and modification of Lf ligand could not increase hemolytic activity. These results
523 suggested that the LB coating could reduce dramatically the hemolysis percentage,
524 and improve significantly the biocompatibility of lf-protocells.

525 The *in vitro* cell viability assays were performed by MTT to evaluate the toxicity
526 of the MSNs and lf-protocells on SH-SY5Y cells. As shown in Fig. S5, over 90 % cell
527 viability was achieved after incubating SH-SY5Y cells with 200 μg/mL of MSNs and
528 lf-protocells respectively for 24 h, while over 85 % cell viability was achieved after
529 incubating SH-SY5Y cells with 500 μg/mL of particles for 24 h. The results suggested
530 that MSNs and lf-protocells possessed low cytotoxicity while the concentration was
531 below 40 μg/mL.

532

533 3.4 Cytotoxicity of curcumin, levodopa and rotenone alone on SH-SY5Y cells

534 The cytotoxicity of curcumin alone, levodopa alone and rotenone alone to
535 SH-SY5Y dopaminergic cell line was evaluated. Cells were treated with various
536 concentrations of curcumin (1, 2, 4 μM), levodopa (20, 40 μM) and rotenone (0.5, 1, 2,
537 4, 10, 20 μM) respectively for 24 h, and the cell viability assays were determined by
538 MTT. As shown in Fig. 2 C-D, curcumin alone below 4 μM did not affect cell
539 viability, while levodopa alone did not affect cell viability at the concentrations of 40
540 μM or lower.

Fig. 2A showed the effect of rotenone on SH-SY5Y cell morphology. Normal SH-SY5Y cells were spindle or polygonal and had mesh connection with circumambient cell. After 24 h treatment, with the increase of concentration, rotenone induced marked cell shrinkage, disappeared connections and loss of whole cells. The above observations indicated that rotenone created the PD cell model successfully and had obvious toxic effect on cellular morphology. As previously reported [37], a significant dose-dependent reduction of rotenone-induced cell viability could be observed. Due to the approximate median lethal dose (LD50) observed at 4 μM.

To investigate the effects of rotenone induction on SH-SY5Y cells, western blot analysis on several important apoptosis mediated signaling pathway proteins was performed. The expression levels of pro-apoptotic factors PARP, Caspase-3, Cleaved Caspase-3, Bax and anti-apoptotic factors Bcl-2 were detected in 10 μM Rot-induced SH-SY5Y cells after 24 h cultivation. Compared with blank group, rotenone significantly increased PARP, Cleaved Caspase-3 and Bax levels and cut down Caspase-3 and Bcl-2 levels, which indicated promotion effect on apoptosis in a dose-dependent manner (Fig. S6A).

Since the typical pathological changes of PD include the deformation of dopaminergic neurons, the aggregation of intracellular α-synaptic nuclear (α-syn) protein and the decrease of TH expression, we measured the expression of α-syn and TH in Rot-induced SH-SY5Y cells.

The results of western blot on TH and α-syn, shown in Fig. S6B, demonstrated that rotenone, compared with blank group, could induce cytotoxicity, and significantly

decreased the level of TH and increased the level of α-syn in a dose-dependent manner.

3.5 Protection of curcumin and levodopa against rotenone-induced cytotoxicity

The cytoprotective effect of curcumin or levodopa against rotenone-induced SH-SY5Y cytotoxicity was determined by pre-treating cells with different concentrations of curcumin or levodopa for 60 min prior to rotenone exposure. Pretreatment with curcumin alone at 1, 2, 4 μM for 60 min prior to rotenone exposure significantly increased the cell viability to 79.2 ± 4.4, 82.6 ± 5.6, 76.9 ± 4.4% of control, respectively, and pretreatment with levodopa alone at 20, 40 μM for 60 min prior to rotenone exposure also immensely enhanced the cell viability to 80.2 ± 4.5, 81.0 ± 4.7% of control, respectively. While the cytoprotective effect of curcumin & levodopa combination against rotenone resulted in dramatic raise in SH-SY5Y cell viability compared with single drug treatment as shown in Fig. 2E-F. Particularly, curcumin and levodopa exerted the highest cytoprotective effect at 2 μM and 40 μM respectively. Therefore, curcumin of 2 μM and levodopa of 40 μM were chosen for the subsequent experiments. The concentration of levodopa and curcumin loaded in C-Lf-Pro, L-Lf-Pro or L/C-Lf-Pro were equivalent to corresponding free drug, respectively.

Fig. 2 Effects of levodopa and curcumin on Rot-induced cytotoxicity.

(A) The cellular morphology of SH-SY5Y cells induced by gradient concentration of Rot. (1) 0

μM Rot (2) 1 μM Rot (3) 2 μM Rot (4) 4 μM Rot (5) 10 μM Rot (6) 20 μM Rot; (**B**) Effect of gradient concentration of Rot on SH-SY5Y cells viability. (mean ± SD; n=6. *** $P < 0.001$ compared with the control group.) (**C-D**) Effects of gradient concentration of curcumin or levodopa on SH-SY5Y cells viability, as well as protection against toxicity induced by 4 μM Rot. (mean ± SD; n=6. *** $P < 0.001$ compared with the 4 μM Rot group.) (**E-F**) Protection of various combinations of gradient concentration of levodopa and curcumin against toxicity induced by 4 μM Rot. (mean ± SD; n=6. *** $P < 0.001$ compared with the 4 μM Rot group. # $P < 0.05$, ## $P < 0.01$ compared between two groups.) Cells were exposed for 24 h and cell viability was determined by MTT assay. Rot: rotenone; C: curcumin; L: levodopa.

3.6 Protection of binary-drug loaded lf-protocells against rotenone-induced cytotoxicity

As shown in Fig. S7, exposure of rotenone (4 μM) led to a dramatic decrease in SH-SY5Y cell viability compared with that in control group. We found that, the pretreatment of unloaded lf-protocells or levodopa loaded lf-protocells, could not increase cell viability. However, curcumin loaded lf-protocells and binary-drug loaded lf-protocells significantly decreased rotenone induced cytotoxicity ($P < 0.01$). Additionally, treatment with binary-drug loaded lf-protocells markedly reduced rotenone-induced cytotoxicity compared with levodopa loaded lf-protocells ($P < 0.05$). In brief, our study showed that binary-drug loaded lf-protocells exerted a significant effect on reduction of cytotoxicity in SH-SY5Y cells activated by rotenone.

607 3.7 Lf-protocells treatment ameliorated oxidative stress in SH-SY5Y cells induced by
608 rotenone
609 3.7.1 Lf-protocells protected against rotenone-induced reactive oxygen species (ROS)
610 production.
611 DCFH-DA, a specific ROS fluorescence probe, was used to analyze whether
612 levodopa and curcumin could inhibit rotenone-induced intracellular ROS generation.
613 The levels of ROS production were determined by the intensity of DCF fluorescence
614 within cells. As shown in Fig. 3A, exposure of rotenone (4 μM) led to a dramatic
615 increase of fluorescence intensity in SH-SY5Y cells compared with that in control
616 group. After the pretreatment of single drug alone, neither curcumin nor levodopa,
617 could decrease the high level of intracellular ROS induced by rotenone. However,
618 co-treatment of curcumin and levodopa (free L/C), as well as treatment of L/C-Lf-Pro,
619 significantly decreased rotenone-induced ROS production ($P < 0.05$, $P < 0.001$,
620 respectively). Interestingly, treatment with L/C-Lf-Pro markedly scavenged
621 rotenone-induced ROS compared with free L/C group ($P < 0.05$), L-Lf-Pro group ($P <$
622 0.001), and C-Lf-Pro group ($P < 0.01$), respectively. In brief, our study showed that
623 L/C-lf-protocells exerted significant effect on reduction of intracellular ROS level in
624 SH-SY5Y cells activated by rotenone.
625
626 3.7.2 Lf-protocells improved the SOD activity.
627 Superoxide dismutase (SOD), as an anti-oxidative defense enzyme, plays a
628 crucial role in maintaining cellular redox homeostasis [38]. Thus, we next determined

629 the effect of lf-protocells on the enzyme activities of SOD. As shown in Fig. 3B,
630 rotenone (4 μM) resulted in a marked decrease in SOD activity of SH-SY5Y cells ($P < 0.01$).
631 Oxidative stress induced by rotenone was confirmed by the reduced expression
632 of SOD. While curcumin & levodopa co-treatment in the form of free drugs (free L/C)
633 and lf-protocells (L/C-Lf-Pro) significantly improved the enzyme activities of SOD
634 reduced by rotenone ($P < 0.01$), and both of them were superior to corresponding
635 single drug treatment ($P < 0.05$). In addition, pretreatment with L/C-Lf-Pro markedly
636 increased the activity of SOD to 93.5 %, the highest among all groups, even though
637 there was no statistical difference compared with free L/C group. In short, our study
638 indicated that L/C-Lf-Pro could efficiently recover the SOD activity impaired by
639 rotenone.
640
641 3.7.3 Lf-protocells improved rotenone-induced GSH depletion.
642 GSH is a tripeptide nonprotein anti-oxidant and redox regulator in brain in which
643 GSH depletion observed probably occurs via oxidative damages caused by increased
644 ROS with significant mitochondrial damage [39]. Based on GSH neutralizing free
645 radicals and reactive oxygen compounds in cells as described above, the assessment
646 of intracellular GSH content should be thought about in further exploration. Since
647 lf-protocells exhibited a profound effect on scavenging Rot-induced intracellular ROS
648 and ameliorating SOD activity, we speculated that lf-protocells could also improve
649 Rot-induced GSH depletion in SH-SY5Y cells.
650 As shown in Fig. 3C, the content of total GSH decreased remarkably after

incubation with rotenone (4 μM) (compared with control group), whereas the total GSH content increased after the pretreatment with levodopa/curcumin for 24 h ($P < 0.01$), as the same trend as that on the improved SOD activity. Noticeably, pretreatment with L/C-Lf-Pro attenuated Rot-induced total GSH depletion, the best among all groups, even though there was no statistical difference compared with free L/C group. These observations implied that L/C-Lf-Pro might provide protection against Rot-induced oxidative damage in SH-SY5Y cells via regulating GSH antioxidant system to cope with oxidative stress.

The occurrence and development of PD are closely related to oxidative stress, which are involved in the process of neuronal deformation in PD. The anti-oxidative therapeutic efficacy of binary-drug loaded lf-protocells were apparently confirmed by SOD and GSH experiment *in vitro*. The results of SOD and GSH were in conformity with the ROS assay. These findings suggested that levodopa and curcumin co-loaded lf-protocells, a novel nanoparticle platform comprised of a Lf-modified lipid bilayer (LB) containing curcumin as its outer membrane and MSNs containing levodopa as its supporting inner core , compared with free levodopa and curcumin, could effectively enhance the level of total GSH and SOD in damaged cells, reduce the oxidative damage, and thus protect cells against oxidative stress, improve the anti-oxidative therapeutic effect for PD.

Fig. 3 Lf-protocells treatment ameliorated oxidative stress in SH-SY5Y cells induced by Rot.

(A) Treatments with lf-protocells protected against Rot-induced ROS in SH-SY5Y cells. The

673 levels of intracellular ROS were quantified by fluorescence with DCF. The fluorescence data were
674 obtained by flow cytometry. **(B)** Effect of lf-protocells on SOD activity reduced by Rot. SOD
675 activity was measured and expressed as U/μg protein. (**C**) Lf-protocells improved Rot-induced
676 total GSH depletion in SH-SY5Y cells. mean ± SD, n=3. * $P < 0.05$, ** $P < 0.01$, *** $P < 0.001$
677 compared with the 4μmol/L Rot group. # $P < 0.05$, ## $P < 0.01$, ### $P < 0.001$, compared between
678 two groups. Rot: rotenone; C: curcumin; L: levodopa; Lf-Pro: lf-protocells.
679
680 3.8 Lf-protocells suppressed rotenone-induced reduction of the MMP
681 As the most important organelle, mitochondria play a key role not only in
682 supplying metabolic energy to cells in the form of ATP via direct participating in a
683 number of metabolic reaction, but also in regulating the signal transmission during the
684 apoptosis of cells [40]. In addition, although electron transport chain in mitochondria
685 is the main source of intracellular ROS, mitochondrial dysfunction, including the
686 collapse of MMP, the membrane non-integrity and membrane oxidative damage and
687 so on, can be aroused by high ROS exposure [41].
688 As we know, the burst of ROS and depletion of intracellular SOD and total GSH
689 can induce the drop of MMP. The collapse of MMP, in turn, can also stimulate ROS
690 generating excessively and the level of SOD and total GSH declining [38]. Since
691 lf-protocells exhibited a profound effect in ameliorating oxidative stress in SH-SY5Y
692 cells induced by rotenone, we postulated that lf-protocells could also ameliorate
693 Rot-induced oxidative damage to membrane and mitochondrial dysfunction.
694 According to the flow cytometry charts, the quantitative data were shown in the

form of bar diagrams. As shown in Fig. 4A, the Rh123 fluorescence intensity of rotenone group was about half of that of control group, a remarkable decrease of fluorescence intensity was observed after treatment with rotenone ($P < 0.001$). Pretreatment with free drugs (including L group, C group and free L/C group), attenuated the decrease of Rot-induced mitochondrial function as reflected by increasing the fluorescence intensity of rotenone group ($P < 0.05$). In addition, pretreatment with L/C-Lf-Pro increased significantly the fluorescence intensity compared with that of free L/C group ($P < 0.05$).

Furtherly, the change of Rh123 fluorescence intensity can be displayed by a visual way with the help of fluorescent confocal microscope (Fig. 4B). The green light intensity characterizing mitochondrial function weakened owing to the addition of rotenone, followed by becoming stronger after treatment with free L/C or L/C-Lf-Pro, which were in accordance with the former results.

Our preliminary data demonstrated that L/C-Lf-Pro enabled to inhibit Rot-induced ROS accumulation. Further research revealed that L/C-Lf-Pro played a role in preventing mitochondrial oxidation due to improving the SOD activity and recovering the level of total GSH, thereby decreasing the oxidative damage to mitochondrial membrane. Since MMP reduction could induce apoptotic signalling downstream involving cytochrome C release from mitochondria and subsequent caspase activation, and could also induce pro-inflammatory signaling during apoptosis [42], L/C-Lf-Pro which suppressed the reduction of MMP might reduce apoptosis. As a consequence, L/C-Lf-Pro were expected to provide protection against

Rot-induced oxidative damage and mitochondrial dysfunction in SH-SY5Y cells.

Fig. 4 Lf-protocells suppressed Rot-induced mitochondrial dysfunction in SH-SY5Y cells. (**A**) Effect of lf-protocells on Rot-induced oxidative damage and mitochondrial dysfunction in SH-SY5Y cells. The mean fluorescence intensity (MFI) was detected in each group. (**B**) The Rh123 accumulation in mitochondria was detected by confocal microscope (scale bar, 25 μm). (mean ± SD; n=3. * $P < 0.05$, ** $P < 0.01$, *** $P < 0.001$ compared with the 4 μmol/L Rot group. # $P < 0.05$, compared between two groups.) Rot: rotenone; C: curcumin; L: levodopa; Lf-Pro: lf-protocells.

3.9 Lf-protocells inhibited rotenone-induced neuronal apoptosis.

To investigate the detailed mechanisms, western blot analysis on several important apoptosis mediated signaling pathway proteins was performed. Anti-apoptotic protein Bcl-2 and pro-apoptotic protein Bax play key roles in the process of apoptosis. The Bcl-2 protein family modulates cell apoptosis by controlling the MMP. Protein Bax is the key component of apoptosis caused by mitochondrial stress and increases membrane permeability after apoptosis stimulation. Over-expression of Bax can accelerate apoptotic death by activating caspase pathway [35]. In addition, once the mitochondrial membrane permeability suffer from damage, Bax may release from the intermembrane space to initiate caspase activation in the cytosol [43]. Protein Caspase-3 has a vital role to play executor of apoptosis and could crack poly ADP-ribose polymerase (PARP). The proenzyme form of Caspase-3

739 is hydrolyzed and activated to a Cleaved Caspase-3 (17 kd subunit + 19 kd subunit).
740 Moreover, PARP is one of the main shearing targets of Caspase-3 *in vivo* and could be
741 used as a marker of apoptosis.

742 Our results, as shown in Fig. 5A, indicated that Bcl-2 and Caspase-3 were
743 up-regulated in both free L/C group and L/C-Lf-Pro group compared with Rot group
744 and single drug groups. Similarly, the expression of Bax, Cleaved Caspase-3 and
745 PARP were down-regulated in both free L/C group and L/C-Lf-Pro group compared
746 with Rot group, and the degree of decrease was markedly enhanced in binary-drug
747 groups compared with single-drug groups. Based on the role of apoptosis mediated
748 signaling pathway proteins as described above, these results suggested that
749 combination of levodopa and curcumin might partially reverse the apoptosis of cells
750 by reducing mitochondrial damage.

751 Since the typical pathological changes of PD include deformation of
752 dopaminergic neurons, aggregation of intracellular α-synaptic nuclear (α-syn) protein
753 and decrease of tyrosine hydroxylase (TH) expression. We measured the expression of
754 PD related proteins using certain experiments.

755 The results of western blot on TH and α-syn showed that rotenone could
756 significantly decrease the level of TH and increase the level of α-syn compared with
757 blank group, while levodopa and curcumin reversed this trend (Fig. 5B). The addition
758 of both free L/C and L/C-Lf-Pro could reduce Rot-introduced cytotoxicity as reflected
759 by increased TH level and decreased α-syn level. Interestingly, the performance of
760 binary-drug group was better than single-drug group. In addition, since TH is the key

761 enzyme in dopamine synthesis, co-delivery of levodopa and curcumin is expected to
762 promote the dopamine synthesis by increasing TH expression. Moreover, the addition
763 of levodopa as a dopaminergic neurotransmitter supplement would further increase
764 dopamine levels. Therefore, the results demonstrated that levodopa and curcumin
765 could protect dopaminergic neurons through decreasing the aggregation of α-syn
766 protein and increasing the activity of TH.

767 Overall, these studies implied that L/C-Lf-Pro pretreatment may alleviate the
768 apoptosis of PD cells and protect dopamine neurons through the following
769 mechanisms: reducing the accumulation of unfolded or misfolded α-syn proteins,
770 enhancing the level of TH and transforming more levodopa into dopamine for
771 supplementing the loss of dopamine in the brain, reducing the mitochondrial damage
772 and dysfunction, down-regulating the expression of Bax protein and up-regulating the
773 expression of Bcl-2, inhibiting the activation of Caspase-3 and thus exerting an
774 anti-apoptotic ability, showing a protective effect in the degenerative changes of
775 dopamine neurons finally.

776

777 **Fig. 5 The effects of levodopa/curcumin and L/C-Lf-Pro on rotenone-induced variation**
778 **in expression of apoptosis related proteins and PD related proteins through western blot**
779 **analysis.**

780 Representative blots on the upper panels, along with bar graph summarizing group data on the
781 bottom panels. (**A**) Expression of apoptosis related proteins in experimental groups. The
782 expressions of Bax, Cleaved Caspase-3, PARP were decreased while the expressions of Bcl-2 and

Caspase-3 were significantly increased by free L/C or L/C-Lf-Pro pretreatment compared with the 10 μmol/L Rot group. Pretreatment with free L/C or L/C-Lf-Pro recovered the imbalanced expression profile of these proteins, protected SH-SY5Y cells against rotenone induced apoptosis. (**B**) Expression of PD related proteins in experimental groups. Pretreatment with free L/C or L/C-Lf-Pro reduced the accumulation of misfolded α-syn and enhanced the level of TH, most obviously compared with other groups. (mean ± SD; n=3. * $P < 0.05$, ** $P < 0.01$, *** $P < 0.001$ compared with the 10 μM Rot group. # $P < 0.05$, ## $P < 0.01$, ### $P < 0.001$ compared between two groups.) Rot: rotenone; C: curcumin; L: levodopa; Lf-Pro: lf-protocells.

3.10 Cellular Uptake

The bEnd.3 cells are the brain microvascular endothelial cells in the BBB. The BBB blocks passage of most drugs. In our study, Lf modified protocells allowed more drugs to pass through BBB by the specific receptor-mediated transport. RBITC was labeled on the inner core of protocells by chemical bond, indicating the location of protocells. Calcein is loaded in protocells by the adsorption of MSNs, indicating the location of loading drugs. The cellular uptake of protocells and their loading drugs was investigated, through labeled with RBITC and Calcein respectively.

The results of cellular uptake were shown in Fig. S8. Only the blue nucleus stained with DAPI were visible in the protocells group, and no other fluorescence was seen. While the lf-protocells group showed distinct red and green fluorescence besides blue. The experimental results indicated that RBITC/Calcein-protocells were hardly internalized by bEnd.3 cells, while the modification of Lf ligand was beneficial to

increase the cellular uptake of protocells and their loading drugs.

3.11 *In Vivo* Research

3.11.1 Biodistribution

Biodistribution of carrier after intraperitoneal injection of Cy5-labeled lf-protocells, unmodified protocells and bare MSNs (denoted as Cy5-lf-protocells, Cy5-protocells, Cy5-MSNs, respectively) were qualitatively assessed by luminescence imaging *in vivo* (Fig. 6A). The results indicated that the injection site (above the right leg of mice) showed strong fluorescence intensity in all experimental groups after injection for 30 min. After 60 min, the fluorescence intensity of lf-protocells group enhanced dramatically in the brain. Interestingly, the brain fluorescence intensity of lf-protocells was further increased, which was much higher than that of bare MSNs and unmodified protocells groups for 120 min. The fluorescence of bare MSNs and unmodified protocells groups concentrated mainly in abdominal cavity, with little or no enrichment in the brain during the whole time of the test.

According to the above results, lf-protocells had specific brain-targeting properties in mice, which may be distributed in the brain at a high concentration due to the modification of active targeting Lf ligand. While either bare MSNs or unmodified protocells had no brain targeting. Noteworthily, Lf is a type of ligand with brain-targeting potential, meanwhile, previous studies have demonstrated that the expression of Lf receptor was increased in the brain of PD patients [44]. Hence, the

high expression of Lf receptor in cerebral microvascular endothelial cells can be utilized to achieve internalization through blood-brain barrier (BBB) by receptor-mediated transport pathway, so as to promote the brain targeting ability of lf-protocells and make them more enriched in the brain of PD patients [45]. Lf-protocells could not only make the brain absorb more levodopa and curcumin, increase the distribution of drugs in the brain compared to free drugs, but also overcome the disadvantage of low bioavailability of curcumin, thus play a better therapeutic role in PD.

3.11.2 L/C-Lf-Pro ameliorated motor function deficits in MPTP-induced PD model mice.

Exposure to MPTP induces a PD-like syndrome such as motor retardation in mice [34]. In the brain, MPTP is converted to MPP^+, which is selectively transported into dopaminergic neuron axon terminals, causing oxidative stress, mitochondrial dysfunction, and cell death [46].

The motor function of PD mice was assessed using the open-field test. Our results indicated that motor function was significantly attenuated from day 1 to day 5 in the MPTP-exposed group, compared with the control group ($P < 0.001$). Neither levodopa nor levodopa/curcumin did affect the improvement of motor function, however, L/C-Pro and L/C-Lf-Pro significantly rescued the reduction of motor function induced by MPTP ($P < 0.05$, $P < 0.01$)(Fig. 6B), and the improvement effect of L/C-Lf-Pro were superior to that of L/C-Pro ($P < 0.05$).

These results suggested that levodopa and curcumin co-loaded lf-protocells had better therapeutic effect on PD-related motor deficits than other groups. One of the possible reasons is that lf-protocells can package drugs into nanoparticles for elevating the bioavailability of drugs. Especially, lf-protocells have an active brain-targeting distribution, which can deliver more drugs into the brain and exploit the advantages to treat PD. But it is important to note that the behavioral judgement of autonomic activity in mice includes a variety of evaluation systems, one of which is selected in this experiment. At the same time, behavioral evaluation is only a part of PD efficacy at the animal level. Therefore, the PD therapy evaluation of lf-protocells needs to be further completed at the animal level in our study.

Because lf-protocells hold several advantages, including drug loading capacity, stability, and the ease of achieving multi-functionality, next studies will explore further improvement of lf-protocells through the addition of design features such as delivering additional synergistic drug combinations, inclusion of other neuroprotective agents.

Fig. 6 *In vivo* experiments on biodistribution and improvement of motor function deficits.

(**A**) *In vivo* imaging of BALB/c-nu mice after administration of Cy5-MSNs, Cy5-protocells, Cy5-lf-protocells at 30, 60, 120 min. (**B**) Effects of L/C-Lf-Pro on locomotor function in MPTP-induced PD model mice. Sum of lines crossing in different experimental groups for five days. (mean ± SD; n=3. ns $P > 0.05$, * $P < 0.05$, ** $P < 0.01$, *** $P < 0.001$ compared with the MPTP group. # $P < 0.05$ compared between two groups.) Cy5-Pro: Cy5-potocells; Cy5-Lf-Pro:

Cy5-lf protocells; Rot: rotenone; C: curcumin; L: levodopa; Lf-Pro: lf-protocells.

Fig. 7 Schematic illustration of binary-drug loaded lf-protocells for treating Parkinson's disease.

(A) Parkinson's disease (PD) is the second most frequent neurodegenerative disease. (B) The pathological hallmark of PD is the characteristic loss of dopaminergic neurons and the appearance of Lewy bodies formed by misfolded and oligomeric α-synuclein. Both mitochondrial dysfunction and oxidative stress are key elements in the pathogenesis of PD. (C) The blood-brain barrier (BBB) limits the delivery of the vast majority of drugs passing from the bloodstream into the brain. (D) Drug delivery system named as binary-drug loaded lf-protocells (L/C-Lf-Pro) shows greatly improved BBB transport efficiency of levodopa and curcumin through lactoferrin receptor-mediated endocytosis. (C) While penetrating into the central nervous system, levodopa and curcumin exhibit neuroprotective effects aganist PD with multiple mechanisms, including enhancing the cell viability, decreasing the expression of a-synuclein, ameliorating oxidative stress and mitochondrial dysfunction.

4. Conclusion

In summary, this work prepared and characterized successfully organic-inorganic composite nanoparticles (namely lf-protocells) which were formed by coating MSNs with lf-modified lipid bilayer for levodopa/curcumin co-delivery to brain, and evaluated therapeutic effects of the binary-drug loaded lf-protocells on PD both *in vitro* and *in vivo*, and explored the possible related mechanism (Fig. 7). As a

mitochondrial protective antioxidant, curcumin combined with levodopa was typically effective for PD treatment. It was worth noting that levodopa not only acted as a dopamine precursor, but also showed a certain degree of anti-oxidative activity. It was reported that levodopa oxidation products prevented H_2O_2-induced oxidative damage to cellular DNA in cultured tissue cells [47]. Compared to that observed following treatment with free levodopa and curcumin, binary-drug loaded lf-protocells (L/C-Lf-Pro) could increase the distribution and bioavailability of drugs in the brain, thereby exhibit better effects on reducing the level of ROS, increasing the level of SOD and total GSH, ameliorating MMP reduction and decreasing the damage of oxidative stress to PD cells. Furthermore, L/C-Lf-Pro treatment not only reduced α-syn accumulation that could cause the formation of Lewy bodies, but also elevated the activity of TH, which is the rate limiting enzyme for the synthesis of dopamine. Presumably, binary-drug loaded lf-protocells (L/C-Lf-Pro) not only converted more levodopa into dopamine to make up for the loss in the brain, but also inhibited MMP reduction, turned off apoptosis signaling pathway, alleviated dopaminergic neuron damage and restored cell survival rate. Loss of dopaminergic neurons leading to striatal dopamine depletion is the core mechanism underlying the cardinal motor features of PD [48]. *In vivo*, the intraperitoneal injection of L/C-Lf-Pro resulted in improvement of motor function deficits, which was evidently superior to those of any other groups. However, more experiments are required to testify the current point of view. For example, an *in vivo* study using MPTP-induced animal models is necessary to be further completed. Overall, L/C-Lf-Pro not only replenished the loss of

dopamine in the brain, but also played the neuroprotective role of antioxidant and repairing injured neurons. The synergy of two different mechanisms can yield a better efficacy for PD, which has been successfully confirmed *in vitro* and *in vivo*. As far as we know, it is the first time that the effect of levodopa & curcumin loaded lf-protocells combination therapy has been applied in PD. The most intriguing thing is the potential application of this approach to other CNS diseases where future lf-protocells could be extended to nanoparticle delivery system for a broad range of drugs, genes or cell-specific targeting [49]. Thus, lf-protocells could offer a basis for future nanocarrier for drug delivery to the CNS.

Declarations

Ethics approval and consent to participate

The study was approved by Ethics Committee of Institute of Medicinal Biotechnology, Chinese Academy of Medical Science & Peking Union Medical College.

Consent for publication

All authors concur with the submission and publication of this paper.

Competing interests

The authors declare that they have no competing interests.

Availability of data and materials

The datasets used and/or analysed during the current study are available from the corresponding author on reasonable request.

Funding

This work was supported by the CAMS Initiative for Innovative Medicine (Grant No. 2017-I2M-1-012)

Contributions

GL and XL led the research. WZ and CL carried out most of experiments and analyzed the data. FY, XN and XM participated in this project. CL and WZ wrote the manuscript, which GL and XL reviewed. All authors read and approved the final manuscript.

Corresponding authors

Correspondence to GL or XL.

Authors' information

[1] Wenkai Zhou, Chang Liu contributed equally to this article.

[2] Institute of Medicinal Biotechnology, Chinese Academy of Medical Science & Peking Union Medical College, Beijing, China.

[3] Department of Pharmaceutics, School of Pharmaceutical Sciences, Peking University, Beijing, China.

[4] Department of Immunology & Centre for Immunotherapy, Institute of Basic Medical Sciences, Peking Union Medical College, Chinese Academy of Medical Sciences, Beijing, China.

Reference

1. Cossu G, Rinaldi R, Colosimo C. The rise and fall of impulse control behavior disorders. Parkinsonism Relat Disord. 2018; 46 Suppl 1S24-S9.
2. Fahn S. The 200-year journey of Parkinson disease: Reflecting on the past and looking towards the future. Parkinsonism Relat Disord. 2018; 46 Suppl 1S1-S5.

3. Calabrese V, Santoro A, Monti D, Crupi R, Di Paola R, Latteri S, Cuzzocrea S, Zappia M, Giordano J, Calabrese EJ, Franceschi C. Aging and Parkinson's Disease: Inflammaging, neuroinflammation and biological remodeling as key factors in pathogenesis. Free Radic Biol Med. 2018; 11580-91.
4. Dias V, Junn E, Mouradian MM. The role of oxidative stress in Parkinson's disease. Journal of Parkinsons Disease. 2013; 3(4):461-91.
5. Hang L, Thundyil J, Lim KL. Mitochondrial dysfunction and Parkinson disease: a Parkin-AMPK alliance in neuroprotection. Ann N Y Acad Sci. 2015; 135037-47.
6. Mosley RL, Benner EJ, Kadiu I, Thomas M, Boska MD, Hasan K, Laurie C, Gendelman HE. Neuroinflammation, Oxidative Stress and the Pathogenesis of Parkinson's Disease. Clinical Neuroscience Research. 2007; 6(5):261-81.
7. Sharma N, Nehru B. Characterization of the lipopolysaccharide induced model of Parkinson's disease: Role of oxidative stress and neuroinflammation. Neurochemistry International. 2015; 8792-105.
8. Szelechowski M, Bétourné A, Monnet Y, Ferré CA, Thouard A, Foret C, Peyrin JM, Hunot S, Gonzalez-Dunia D. A viral peptide that targets mitochondria protects against neuronal degeneration in models of Parkinson's disease. Nat Commun. 2014; 55181.
9. Wu HM, Li T, Wang ZF, Huang SS, Shao ZQ, Wang K, Zhong HQ, Chen SF, Zhang X, Zhu JH. Mitochondrial DNA variants modulate genetic susceptibility to Parkinson's disease in Han Chinese. Neurobiol Dis. 2018; 11417-23.
10. Franco MR, Viana TF, Biscaia S, Bártolo P. Levodopa Incorporation in Alginate Membranes for Drug Delivery Studies. Advanced Materials Research. 2013; 749423-8.
11. Kestenbaum M, Fahn S. Safety of IPX066 , an extended release carbidopa-levodopa formulation, for the treatment of Parkinson's disease. Expert Opin Drug Saf. 2015; 14(5):761-7.
12. Xue Z, Wen Z, Li-da D, Li G, Guan-hua D. Advances in anti-Parkinson's disease drugs and their related pharmacological targets. J Int Pharm Res. 2016; 43(01):87-96.
13. Bollimpelli VS, Kumar P, Kumari S, Kondapi AK. Neuroprotective effect of curcumin-loaded lactoferrin nano particles against rotenone induced neurotoxicity. Neurochem Int. 2016; 9537-45.
14. Harish G, Venkateshappa C, Mythri RB, Dubey SK, Mishra K, Singh N, Vali S, Bharath MM. Bioconjugates of curcumin display improved protection against glutathione depletion mediated oxidative stress in a dopaminergic neuronal cell line: Implications for Parkinson's disease. Bioorg Med Chem. 2010; 18(7):2631-8.
15. Ortiz-Ortiz MA, Morán JM, Ruiz-Mesa LM, Niso-Santano M, Bravo-SanPedro JM, Gómez-Sánchez R, González-Polo RA, Fuentes JM. Curcumin exposure induces expression of the Parkinson's disease-associated leucine-rich repeat kinase 2 (LRRK2) in rat mesencephalic cells. Neurosci Lett. 2010; 468(2):120-4.
16. Jagatha B, Mythri RB, Vali S, Bharath MM. Curcumin treatment alleviates the effects of glutathione depletion in vitro and in vivo: therapeutic implications for Parkinson's disease explained via in silico studies. Free Radic Biol Med. 2008; 44(5):907-17.
17. Kulkarni AP, Kellaway LA, Lahiri DK, Kotwal GJ. Neuroprotection from complement-mediated inflammatory damage. Ann N Y Acad Sci. 2004; 1035147-64.
18. Liu Z, Yu Y, Li X, Ross CA, Smith WW. Curcumin protects against A53T alpha-synuclein-induced toxicity in a PC12 inducible cell model for Parkinsonism. Pharmacol

Res. 2011; 63(5):439-44.
19. Wang J, Du XX, Jiang H, Xie JX. Curcumin attenuates 6-hydroxydopamine-induced cytotoxicity by anti-oxidation and nuclear factor-kappa B modulation in MES23.5 cells. Biochem Pharmacol. 2009; 78(2):178-83.
20. Lee WH, Loo CY, Bebawy M, Luk F, Mason RS, Rohanizadeh R. Curcumin and its derivatives: their application in neuropharmacology and neuroscience in the 21st century. Curr Neuropharmacol. 2013; 11(4):338-78.
21. Monroy A, Lithgow GJ, Alavez S. Curcumin and neurodegenerative diseases. Biofactors. 2013; 39(1):122-32.
22. Butler KS, Durfee PN, Theron C, Ashley CE, Carnes EC, Brinker CJ. Protocells: Modular Mesoporous Silica Nanoparticle-Supported Lipid Bilayers for Drug Delivery. Small. 2016; 12(16):2173-85.
23. Liu J, Stace-Naughton A, Jiang X, Brinker CJ. Porous nanoparticle supported lipid bilayers (protocells) as delivery vehicles. J Am Chem Soc. 2009; 131(4):1354-5.
24. Ashley CE, Carnes EC, Phillips GK, Padilla D, Durfee PN, Brown PA, Hanna TN, Liu J, Phillips B, Carter MB, et al. The targeted delivery of multicomponent cargos to cancer cells by nanoporous particle-supported lipid bilayers. Nat Mater. 2011; 10(5):389-97.
25. Chen F, Hong H, Zhang Y, Valdovinos HF, Shi S, Kwon GS, Theuer CP, Barnhart TE, Cai W. In vivo tumor targeting and image-guided drug delivery with antibody-conjugated, radiolabeled mesoporous silica nanoparticles. ACS Nano. 2013; 7(10):9027-39.
26. Mekaru H, Lu J, Tamanoi F. Development of mesoporous silica-based nanoparticles with controlled release capability for cancer therapy. Adv Drug Deliv Rev. 2015; 9540-9.
27. Meng H, Mai WX, Zhang H, Xue M, Xia T, Lin S, Wang X, Zhao Y, Ji Z, Zink JI, Nel AE. Codelivery of an optimal drug/siRNA combination using mesoporous silica nanoparticles to overcome drug resistance in breast cancer in vitro and in vivo. ACS Nano. 2013; 7(2):994-1005.
28. Ye Y, Sun Y, Zhao H, Lan M, Gao F, Song C, Lou K, Li H, Wang W. A novel lactoferrin-modified beta-cyclodextrin nanocarrier for brain-targeting drug delivery. Int J Pharm. 2013; 458(1):110-7.
29. C B. Physiology: Double function at the blood-brain barrier. Nature. 2014; 509(7501):432-3.
30. BA F, N N, P D, G S, A M-P, A P, B L, N K, JJ H, Y A. Expression of lactoferrin receptors is increased in the mesencephalon of patients with Parkinson disease. Proceedings of the National Academy of Sciences of the United States of America. 1995; 92(21):9603-7.
31. T K, I T, T Y, DG W, PL M. Lactotransferrin immunocytochemistry in Alzheimer and normal human brain. The American journal of pathology. 1993; 142(5):1574-85.
32. Zhai H, Wang Y, Wang M, Liu S, Yu F, Gao C, Li G, Wu Q. Construction of a Glutathione-Responsive and Silica-Based Nanocomposite for Controlled Release of Chelator Dimercaptosuccinic Acid. Int J Mol Sci. 2018; 19(12):E3790.
33. Meng H, Wang M, Liu H, Liu X, Situ A, Wu B, Ji Z, Chang CH, Nel AE. Use of a lipid-coated mesoporous silica nanoparticle platform for synergistic gemcitabine and paclitaxel delivery to human pancreatic cancer in mice. ACS Nano. 2015; 9(4):3540-57.
34. Li Y, Perry T, Kindy MS, Harvey BK, Tweedie D, Holloway HW, Powers K, Shen H, Egan JM, Sambamurti K, et al. GLP-1 receptor stimulation preserves primary cortical and dopaminergic neurons in cellular and rodent models of stroke and Parkinsonism. Proc Natl Acad Sci USA. 2009; 106(4):1285-90.

35. Kim MH, Na HK, Kim YK, Ryoo SR, Cho HS, Lee KE, Jeon H, Ryoo R, Min DH. Facile synthesis of monodispersed mesoporous silica nanoparticles with ultralarge pores and their application in gene delivery. ACS Nano. 2011; 5(5):3568-76.
36. Roggers RA, Joglekar M, Valenstein JS, Trewyn BG. Mimicking red blood cell lipid membrane to enhance the hemocompatibility of large-pore mesoporous silica. ACS Appl Mater Interfaces. 2014; 6(3):1675-81.
37. Kundu P, Das M, Tripathy K, Sahoo SK. Delivery of Dual Drug Loaded Lipid Based Nanoparticles across the Blood-Brain Barrier Impart Enhanced Neuroprotection in a Rotenone Induced Mouse Model of Parkinson's Disease. ACS Chem Neurosci. 2016; 7(12):1658-70.
38. Chen W, Su H, Xu Y, Jin C. In vitro gastrointestinal digestion promotes the protective effect of blackberry extract against acrylamide-induced oxidative stress. Sci Rep. 2017; 740514.
39. Perricone C, De Carolis C, Perricone R. Glutathione: a key player in autoimmunity. Autoimmun Rev. 2009; 8(8):697-701.
40. Martinou J-C, Youle Richard J. Mitochondria in Apoptosis: Bcl-2 Family Members and Mitochondrial Dynamics. Developmental Cell. 2011; 21(1):92-101.
41. Circu ML, Aw TY. Reactive oxygen species, cellular redox systems, and apoptosis. Free Radical Biology and Medicine. 2010; 48(6):749-62.
42. Bock FJ, Tait SWG. Mitochondria as multifaceted regulators of cell death. Nature reviews Molecular cell biology. 2020; 21(2):85-100.
43. Skommer J, Brittain T, Raychaudhuri S. Bcl-2 inhibits apoptosis by increasing the time-to-death and intrinsic cell-to-cell variations in the mitochondrial pathway of cell death. Apoptosis. 2010; 15(10):1223-33.
44. Huang RQ, Ke WL, Qu YH, Zhu JH, Pei YY, Jiang C. Characterization of lactoferrin receptor in brain endothelial capillary cells and mouse brain. J Biomed Sci. 2007; 14(1):121-8.
45. Fang F, Zou D, Wang W, Yin Y, Yin T, Hao S, Wang B, Wang G, Wang Y. Non-invasive approaches for drug delivery to the brain based on the receptor mediated transport. Mater Sci Eng C Mater Biol Appl. 2017; 761316-27.
46. Javitch JA, D'Amato RJ, Strittmatter SM, Snyder SH. Parkinsonism-inducing neurotoxin, N-methyl-4-phenyl-1,2,3,6 -tetrahydropyridine: uptake of the metabolite N-methyl-4-phenylpyridine by dopamine neurons explains selective toxicity. Proc Natl Acad Sci USA. 1985; 82(7):2173-7.
47. Shi Y-l, Benzie IFF, Buswell JA. L-DOPA oxidation products prevent H2O2-induced oxidative damage to cellular DNA. Life sciences. 2002; 71(26):3047-57.
48. Poewe W, Seppi K, Tanner CM, Halliday GM, Brundin P, Volkmann J, Schrag AE, Lang AE. Parkinson disease. Nat Rev Dis Primers. 2017; 317013.
49. Dengler EC, Liu J, Kerwin A, Torres S, Olcott CM, Bowman BN, Armijo L, Gentry K, Wilkerson J, Wallace J, et al. Mesoporous silica-supported lipid bilayers (protocells) for DNA cargo delivery to the spinal cord. J Control Release. 2013; 168(2):209-24.

Figures

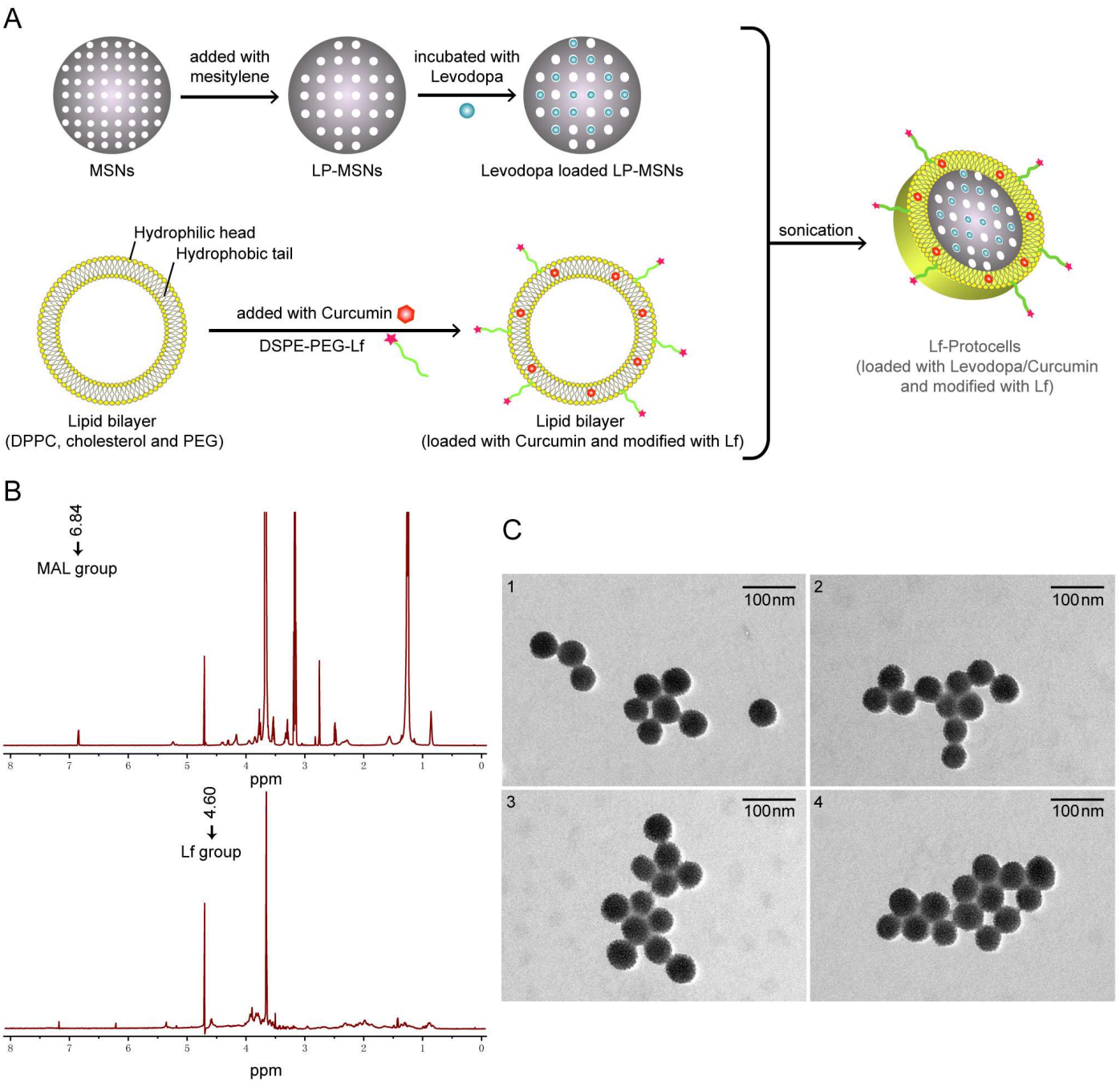

Figure 1

Preparation and characterization of lf-protocells.

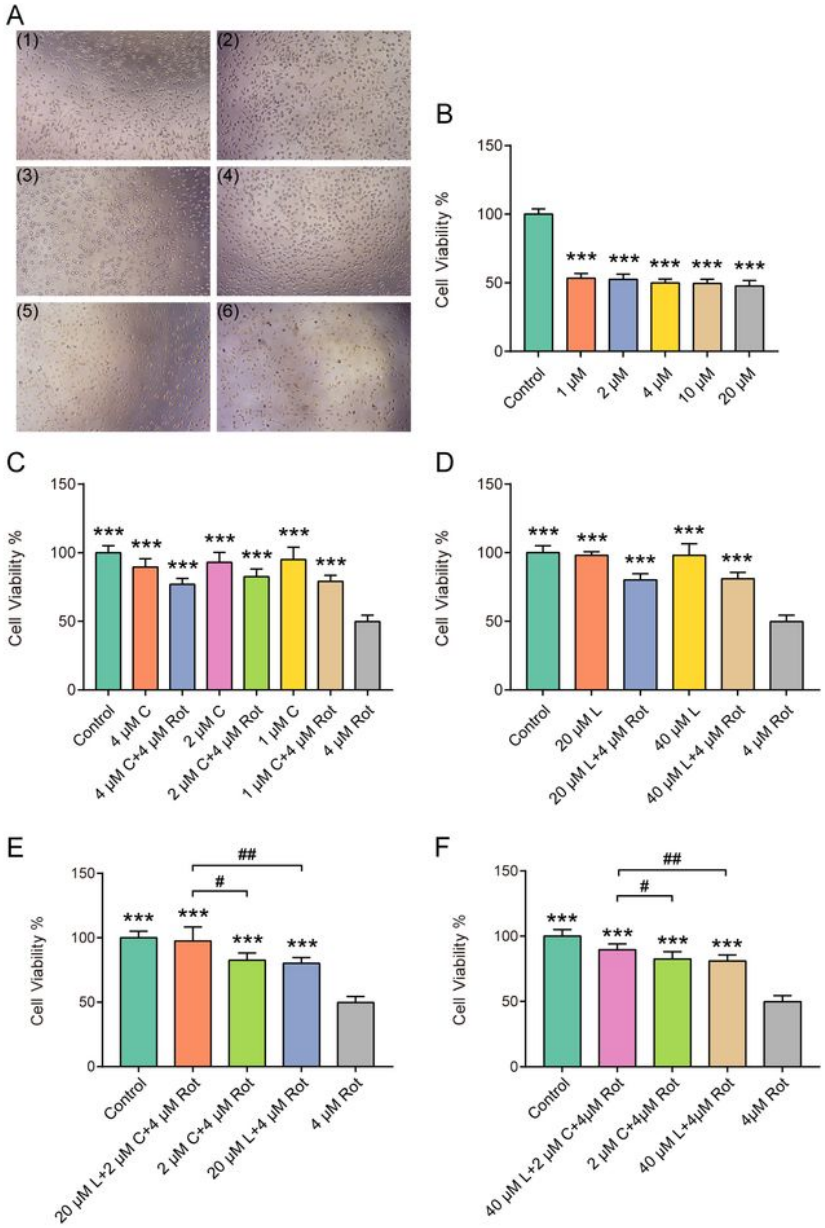

Figure 2

Effects of levodopa and curcumin on Rot-induced cytotoxicity.

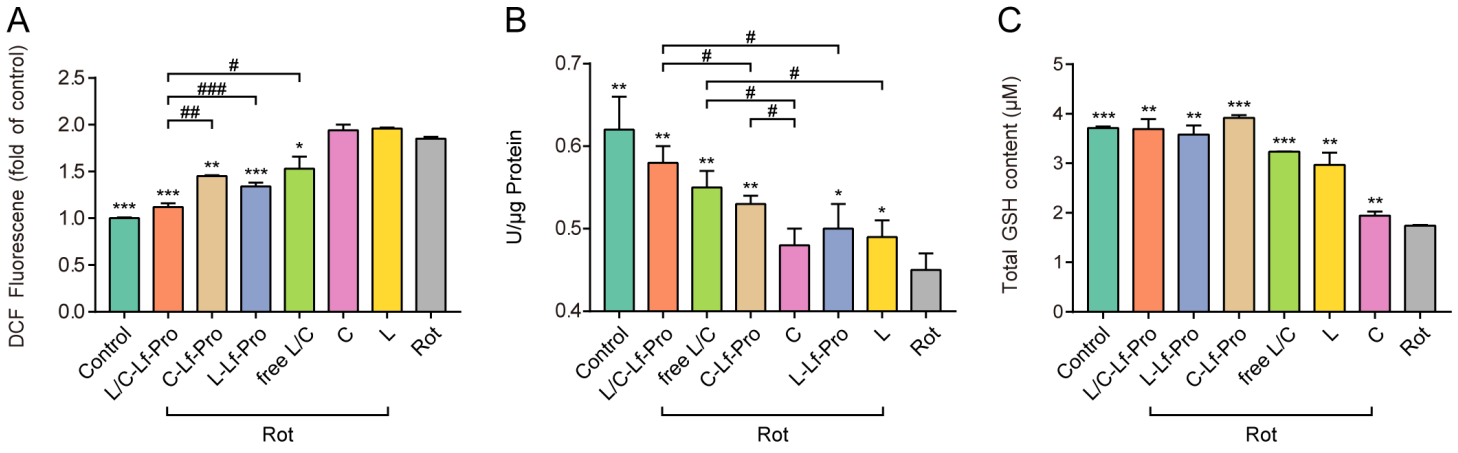

Figure 3

Lf-protocells treatment ameliorated oxidative stress in SH-SY5Y cells induced by Rot.

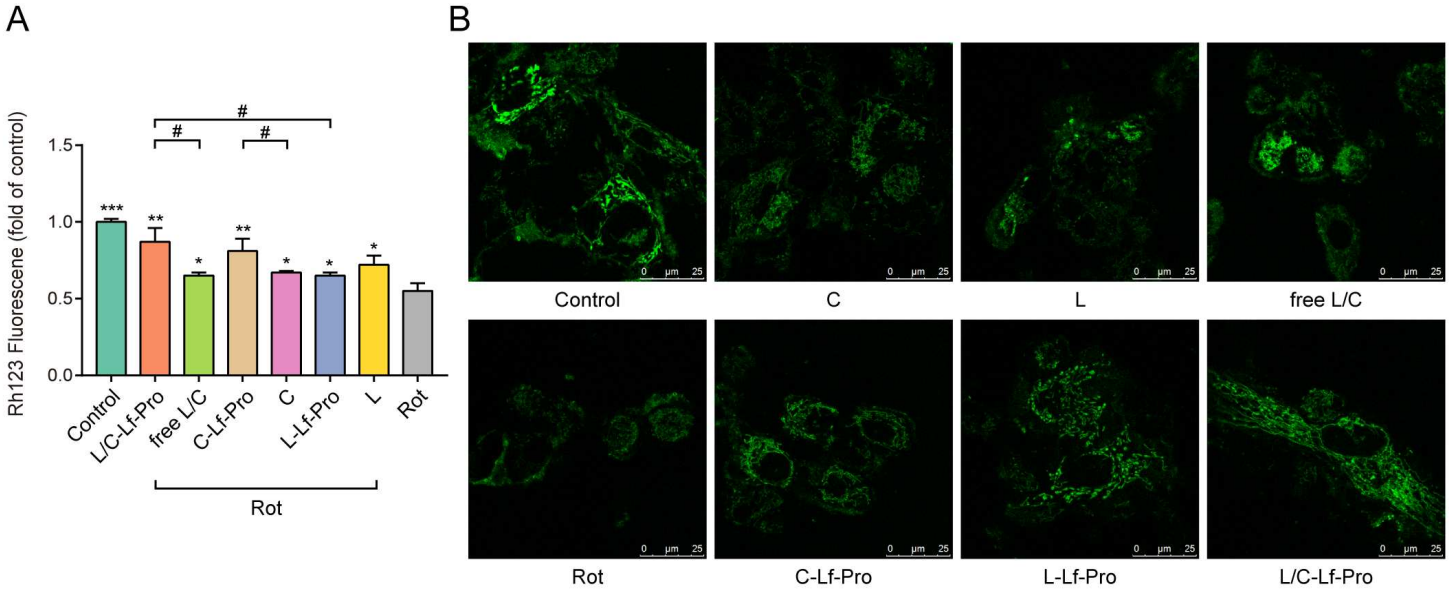

Figure 4

Lf-protocells suppressed Rot-induced mitochondrial dysfunction in SH-SY5Y cells.

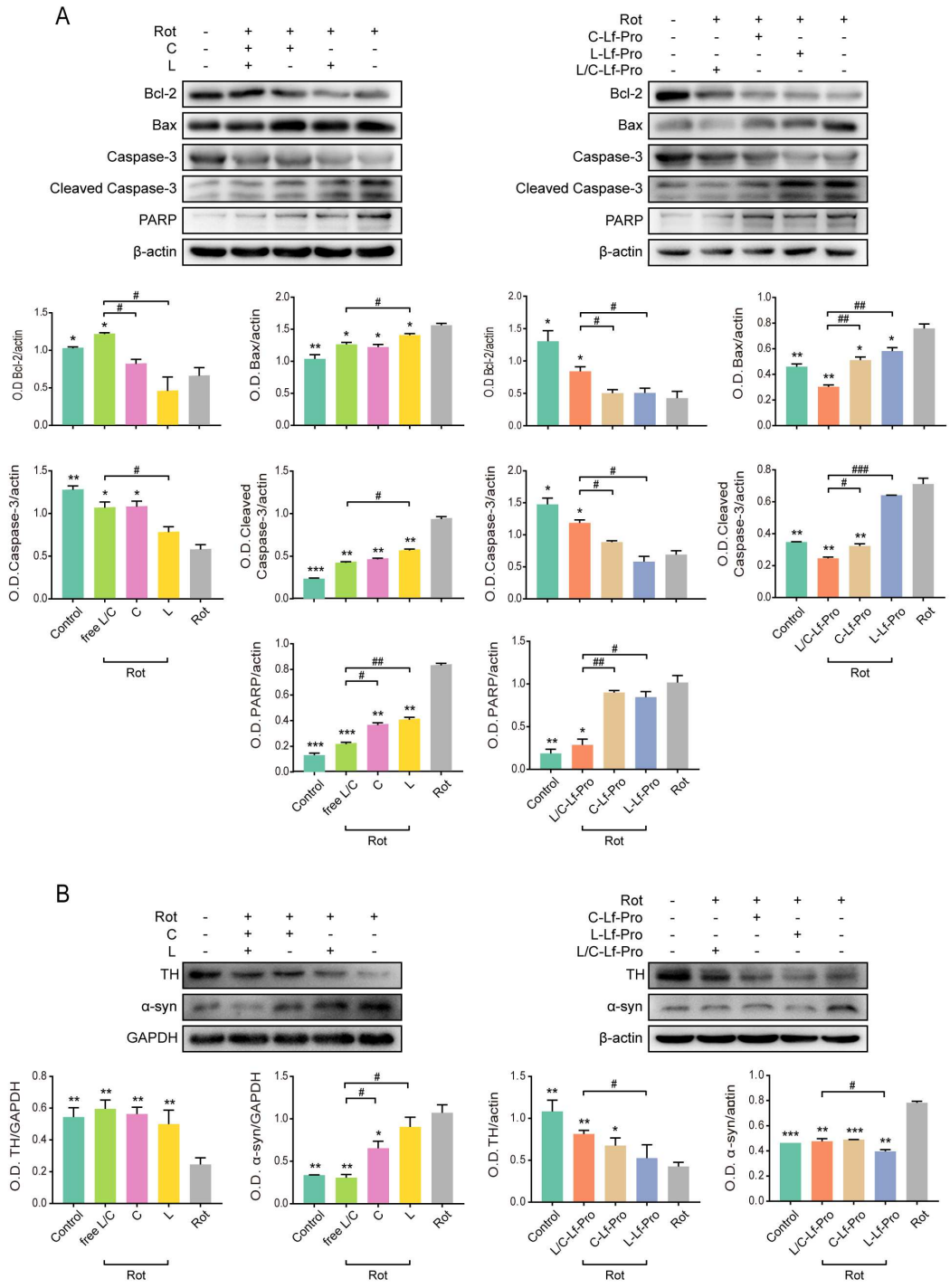

Figure 5

The effects of levodopa/curcumin and L/C-Lf-Pro on rotenone-induced variation in expression of apoptosis related proteins and PD related proteins through western blot analysis.

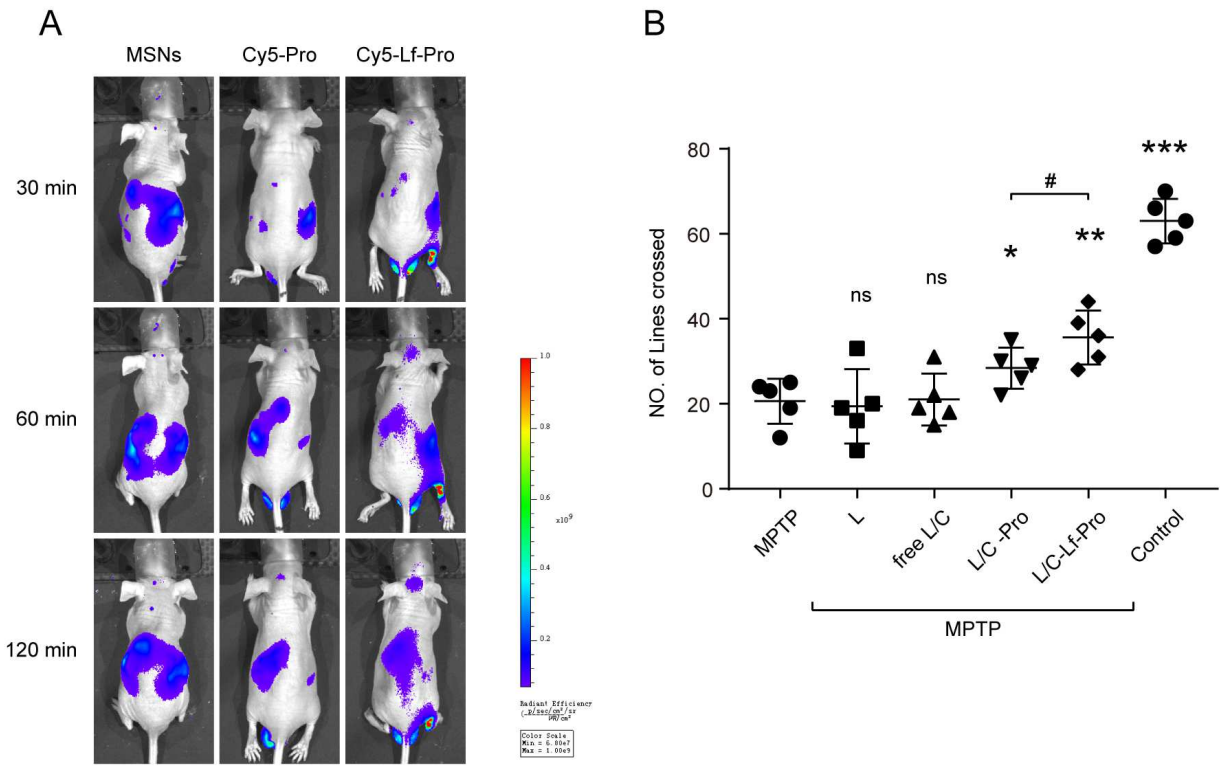

Figure 6

In vivo experiments on biodistribution and improvement of motor function deficits.

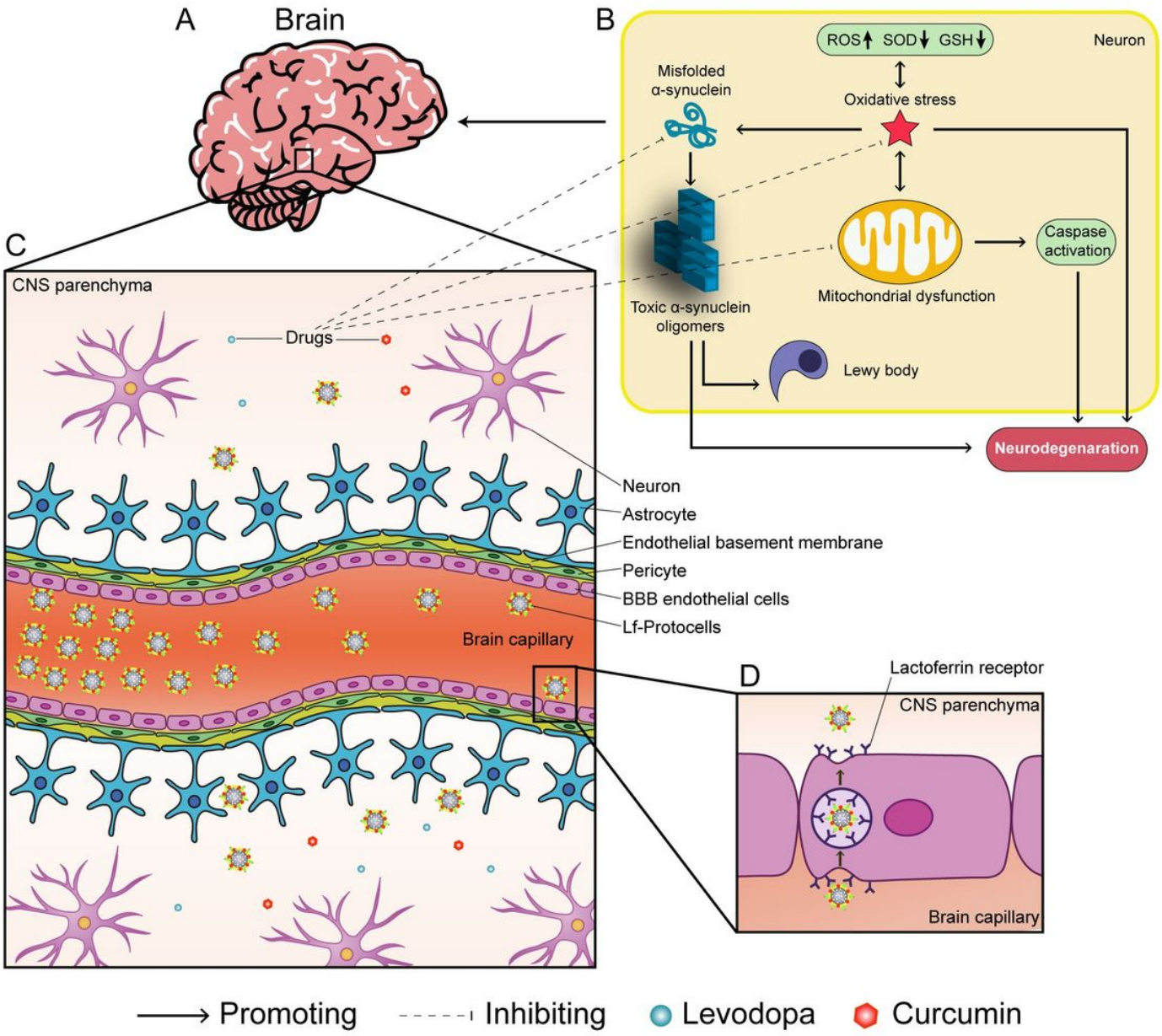

Figure 7

Schematic illustration of binary-drug loaded lf-protocells for treating Parkinson's disease.

Supplementary Files

This is a list of supplementary files associated with this preprint. Click to download.

- supplement.docx